XV Reunión de Trabajo en Procesamiento de la Información y Control, 16 al 20 de septiembre de 2013

A Robust Wireless OFDM Echo Cancellation System

Micael Bernhardt,[†‡] Fernando H. Gregorio[†] and Juan E. Cousseau[†]

† *IIIE-CONICET-Departamento de Ingeniería Eléctrica y Computadoras*
Universidad Nacional del Sur. Av. Alem 1253, Bahía Blanca, Argentina.
mbernhardt@iiie-conicet.gob.ar fernando.gregorio@uns.edu.ar jcousseau@uns.edu.ar
‡*Departamento de Ingeniería Electrónica, Facultad de Ingeniería, Universidad Nacional de Misiones*
Juan Manuel de Rosas 325, Oberá, Misiones, Argentina.

***Abstract*— In this paper, we introduce an echo cancellation technique for full-duplex wireless Orthogonal Frequency Division Modulation (OFDM) communication. The novelty of the work is related to improvements in the models to compensate far-end channel and transmitter front-end, not considered before. Interference cancellation is based on Least Squares (LS) algorithm performed in two successive stages, while far-end channel estimation is accomplished by a training symbol. Using simulation results, we show that the self-interference suppression achieved by our technique increases the system capacity up to levels close to the equivalent of a transmission without interference.**

***Keywords*— Echo cancellation, wireless, OFDM, full-duplex, self-interference.**

1 INTRODUCTION

Orthogonal Frequency Division Multiplexing (OFDM) is a widely used modulation technique for broadband wireless communication systems [1, 2]. However, upon several advantages, OFDM is very sensitive to different system distortions associated to the RF front-end. In recent years, there has been wide interest in development of techniques to mitigate front-end imperfections, and thereby to reduce the performance degradation in those systems [3].

On the other hand, less attention has been paid to use more efficiently the wireless spectrum by means of full-duplex transmissions. Employing a single channel for up- and downlink communications could potentially double the system capacity, compared to more common Frequency Division Duplexing (FDD) and Time Division Duplexing (TDD) technologies [4, 5] used frequently in popular standards (WiFi and/or WIMAX, for example).

Some recent works show that wireless full-duplex operation is feasible [6, 7]. Cancellation of the self-interference in the digital domain only is strongly restricted by the large power differences between the interferer and the signal of interest and the limited dynamic range of analog-to-digital converters (ADC) [8]. Nevertheless, combination of different passive and/or active cancellation techniques prior to ADC, can reduce the amount of interference suppression required to be performed in digital domain [9]. In [7], passive cancellation by means of antenna placement mitigates self-interference by ≈20 dB, while a RF interference cancellation integrated circuit contributes with another 20 dB of suppression. Two RF techniques are used in [6]: the first one is a balun cancellation that attains 40-45 dB of attenuation, and the second one is based on the same RF interference cancellation integrated circuit mentioned earlier.

In this paper, we present a robust digital-domain baseband echo cancellation technique for wireless OFDM communication systems, based on near- and far-end channel estimation. The self-interference is modeled using a transmitter output reference signal, and subtracted to the received signal. Near-end channel and interference estimation are obtained in two stages. Different to previous approaches, the far-end channel parameters and transmitter I/Q imbalance are jointly estimated using a training symbol, which enables communication between signals affected by this degradation phenomenon.

In the next section of this paper, we introduce our system model, while in section 3 the echo cancellation technique is presented and discussed. Simulation results are showed in section 4. Finally, our conclusions are presented in section 5.

2 SYSTEM MODEL

The system model consists of the transceiver structure, OFDM modulator, wireless channel, I/Q imbalance and interference signal models.

2.1 Transceiver structure

In the system model we consider a pair of OFDM transceivers operating simultaneously on the same frequency band, as illustrated in Fig. 1. At any of the receiver antennas, the detected signal r consists

of the superposition of the far-end transmitted message t_{FE} and the near-end self-interference t_{NE}, plus additive white Gaussian noise (AWGN) z.

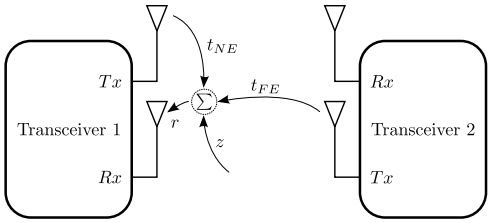

Figure 1: Transceivers operating simultaneously on the same frequency band. The received signal r is the sum of the near- and far-end transmitted signals t_{NE} and t_{FE}, plus AWGN z.

2.2 OFDM modulation

OFDM modulation is performed using the following expression [10]

$$s\left[n\right] = \frac{1}{N}\sum_{k=0}^{N-1} S\left[k\right] e^{j\frac{2\pi}{N}kn},$$

where $s\left[n\right]$ are the samples of the OFDM modulated signal, obtained by applying Inverse Discrete Fourier Transform (IDFT) to the symbols $S\left[k\right]$ transmitted in each of the N subcarriers. Using the Discrete Fourier Transform (DFT) it is possible to recover the symbols transmitted in each tone. The insertion of a cyclic prefix (CP) at the beginning of each OFDM block, consisting of the latest L_{CP} samples of the OFDM block, allows the use of Inverse Fast Fourier Transform (IFFT) and Fast Fourier Transform (FFT) algorithms to perform efficiently modulation and demodulation, respectively. The only condition to accomplish this is $L_{CP} \geq L$, with L the channel impulse response length.

2.3 Wireless channel

The signals are transmitted over a multipath Rayleigh fading channel, whose impulse response in discrete time $h\left[n\right]$ can be modeled, according to [11], using the expression

$$h\left[n\right] = \sum_{i=1}^{L} a_i\left[n\right]\delta\left[n-\tau_i\right], \tag{1}$$

where $a_i\left[n\right]$ and τ_i are the attenuation factors and propagation delays associated with each of the paths for the arriving signal. In this paper, we consider a channel with L different paths and uniformly spaced propagation delays, $\tau_i = (i-1)\,T_s$, with $1 \leq i \leq L$ and T_s equal to the sampling period. The attenuation factors are assumed to be constant within one or more OFDM symbols.

The received signal power is modeled as inversely proportional to the fourth power of the distance between the transmit and receive antennas [12].

2.4 I/Q imbalance

The transmitter I/Q imbalance is originated by the amplitude and phase difference between the signals in the in-phase and quadrature branches at the transmitter front-end. This phenomenon can be characterized by [13]

$$x_{IQ}\left[n\right] = \alpha x\left[n\right] + \beta x^{*}\left[n\right], \tag{2}$$

where $\mathbf{x}$ is the perfect balanced transmit signal, $\mathbf{x}_{IQ}$ is the I/Q imbalance affected signal, and α and β are parameters defined by the amplitude difference ϵ and phase orthogonality mismatch $\Delta\phi$, and can be obtained by

$$\alpha = \frac{1+\epsilon\cdot e^{j\Delta\phi}}{2}, \qquad \beta = \frac{1-\epsilon\cdot e^{j\Delta\phi}}{2}.$$

The effects of transmitter I/Q imbalance and channel filtering can be coupled. If $x\left[n\right]$ is the transmitted signal with perfect I/Q balance in discrete time domain n, and $y\left[n\right]$ the I/Q imbalance affected signal at the output of the channel, following (2), and ignoring noise effect, we can write

$$y\left[n\right] = h\left[n\right] \star \left(\alpha x\left[n\right] + \beta x^{*}\left[n\right]\right), \tag{3}$$

where $h\left[n\right]$ is the channel impulse response, and $\star$ denotes convolution. If we take the Discrete Fourier Transform (DFT) of (3), we obtain

$$\begin{aligned} Y\left[k\right] &= H\left[k\right]\cdot\left(\alpha X\left[k\right] + \beta X^{\#}\left[k\right]\right) \\ &= \alpha H\left[k\right] X\left[k\right] + \beta H\left[k\right] X^{\#}\left[k\right] \\ &= H_{\alpha}\left[k\right] X\left[k\right] + H_{\beta}\left[k\right] X^{\#}\left[k\right] \end{aligned} \tag{4}$$

where $X^{\#}\left[k\right]$ is the conjugated OFDM symbol mirrored over the carriers, as given by

$$X^{\#}\left[k\right] = X^{*}\left[-i\right],\ i = \mathrm{mod}\left(N-k+2, N\right), \tag{5}$$

where mod is the module operation, and $1 \leq k \leq N$. The total effect of transmitter I/Q imbalance and channel filtering is modeled by (4) in the frequency domain.

2.5 Baseband signal and interference model

The N samples per OFDM symbol of the received signal $\mathbf{r} = \left[r_0, r_1, \ldots, r_{N-1}\right]^T$ can be obtained by

$$\mathbf{r} = \mathbf{X}_{NE}\mathbf{h}_{NE} + \mathbf{F}\mathbf{X}_{FE}\mathbf{h}_{FE} + \mathbf{z}, \tag{6}$$

where $\mathbf{z} = \left[z_0, z_1, \ldots, z_{N-1}\right]^T$ is complex AWGN, $\mathbf{h}_{FE} = \left[h_{FE,0}, h_{FE,1}, \ldots, h_{FE,L-1}\right]^T$ and $\mathbf{h}_{NE} = \left[h_{NE,0}, h_{NE,1}, \ldots, h_{NE,L-1}\right]^T$ are the far-end and near-end channel impulse responses, each of length L.

$\mathbf{X}_{NE}$ and $\mathbf{X}_{FE}$ are defined by

$$\mathbf{X}_{NE} = \begin{bmatrix} x_0^{NE} & 0 & \cdots & 0 \\ x_1^{NE} & x_0^{NE} & \cdots & 0 \\ x_2^{NE} & x_1^{NE} & \cdots & 0 \\ \vdots & \vdots & \ddots & \vdots \\ x_{N-1}^{NE} & x_{N-2}^{NE} & \cdots & x_{N-(L-1)}^{NE} \end{bmatrix}$$

$$\mathbf{X}_{FE} = \begin{bmatrix} x_0^{FE} & 0 & \cdots & 0 \\ x_1^{FE} & x_0^{FE} & \cdots & 0 \\ x_2^{FE} & x_1^{FE} & \cdots & 0 \\ \vdots & \vdots & \ddots & \vdots \\ x_{N-1}^{FE} & x_{N-2}^{FE} & \cdots & x_{N-(L-1)}^{FE} \end{bmatrix},$$

where x_i^{NE} and x_i^{FE} are the $i-th$ samples of the near-end and far-end transmitted symbols, respectively. $\mathbf{F}$ models the effect of carrier frequency difference Δf between transmitter and receiver, and is defined by

$$\mathbf{F} = \text{diag}\left[1, e^{j\Delta\omega T_s}, e^{j\Delta\omega 2T_s}, \ldots, e^{j\Delta\omega(N-1)T_s}\right], \tag{7}$$

where $\Delta\omega = 2\pi\Delta f$, and T_s is the sampling interval.

3 ECHO CANCELLATION

Echo cancellation is implemented in two stages as in [14]. The first one produces a good approximation to the far-end transmitted signal that enables data recovery with sufficient accuracy. This data is remodulated at the receiver to obtain a far-end signal model, used in the second stage of echo cancellation to improve interference estimation. Different to [14], our technique uses a training symbol to estimate the far-end transmitter I/Q imbalance jointly to the wireless channel, permitting communications when both near- and far-end transmitted signals are affected by this degradation phenomenon. In the next two subsections we offer a detailed description of how echo cancellation and far-end channel and transmitter I/Q imbalance estimation are obtained.

3.1 Near-End self-interference cancellation technique

The structure of the digital baseband interference canceler is shown in Fig. 2. For simplicity, other interference cancellation methods like antenna placement or RF techniques are not shown.

A reference signal $x_{NE}[n]$ for echo estimation is obtained using a coupler attached to the near-end transmit antenna. This way, degradations caused by the near-end transmitter front-end, like I/Q imbalance, have not to be taken into account by the corresponding channel model. The first compensation stage considers that the interference signal $h_{NE}[n] \star x_{NE}[n]$ arrives at the receive antenna with more power than the far-end signal, because normally the distance from the receiving antenna to the far-end transmitter is greater than the distance to the near-end transmitting antenna. With this assumption, from (6) we can write

$$\mathbf{r} \approx \mathbf{X}_{NE}\mathbf{h}_{NE} + \mathbf{z}, \tag{8}$$

and the near-end channel impulse response can be estimated by Least Squares (LS) method as follows

$$\hat{\mathbf{h}}_{NE} = \left(\mathbf{X}_{NE}^H \mathbf{X}_{NE}\right)^{-1} \mathbf{X}_{NE}^H \mathbf{r}. \tag{9}$$

After filtering the reference signal obtained at the near-end transmitter antenna with this channel impulse response model, we obtain an interference estimation that can be subtracted from the received signal $\mathbf{r}$. This near-end channel and self-interference estimation is improved in the second stage by reconstructing the far-end transmitted signal from the data detected after the first stage. For this new cancellation, after (6) we can write

$$\begin{aligned} \mathbf{r} &\approx \mathbf{X}_{NE}\mathbf{h}_{NE} + \mathbf{F}\hat{\mathbf{X}}_{FE}\hat{\mathbf{h}}_{FE} + \mathbf{z} \\ &\approx \begin{bmatrix} \mathbf{X}_{NE} & \mathbf{F}\hat{\mathbf{X}}_{FE} \end{bmatrix} \begin{bmatrix} \mathbf{h}_{NE} \\ \hat{\mathbf{h}}_{FE} \end{bmatrix} + \mathbf{z} \qquad (10) \\ &\approx \mathbf{A} \begin{bmatrix} \mathbf{h}_{NE} \\ \hat{\mathbf{h}}_{FE} \end{bmatrix} + \mathbf{z} \qquad (11) \end{aligned}$$

where $\hat{\mathbf{X}}_{FE}$ is the received data remodulated at the receiver, and $\hat{\mathbf{h}}_{FE}$ is the far-end channel estimation obtained as we describe in next subsection. The Carrier Frequency Offset (CFO) modeled by $\mathbf{F}$ is supposed to be known at the receiver, allowing exact compensation when demodulating the received signal, and reproducing its effect on the remodulated signal. From (11) we can obtain a new near-end channel estimation using LS, as given by

$$\hat{\mathbf{h}}_{NE} = \left(\mathbf{A}^H \mathbf{A}\right)^{-1} \mathbf{A}^H \mathbf{r}. \tag{12}$$

This new estimation allows us to recalculate self-interference, and improve its cancellation.

3.2 Far-end channel and transmitter I/Q imbalance estimation

Despite that I/Q imbalance at the near-end transmitter has not to be taken into account since the reference signal used for the interference cancellation suffers the same degradation as the transmitted signal, this situation changes as ones considers the transmission at the other end of the link. If both transceivers share the same technological limitations, it is expected that their transmitted signals suffer similar imperfections. The effect of far-end transmitter I/Q imbalance has to be estimated, for both compensation prior to demodulation and modeling of the far-end signal at the second stage of the self-interference cancellation. A simple way to estimate

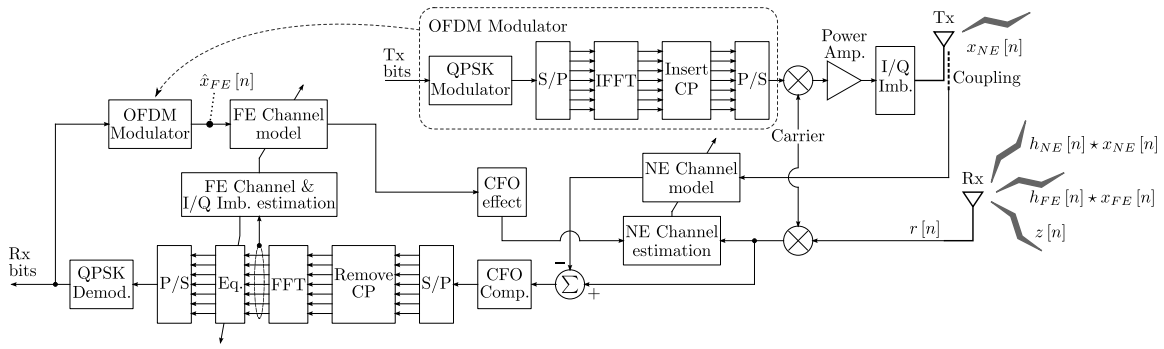

Figure 2: Block diagram of a transceiver with echo cancellation.

the degradation is using a training OFDM symbol at the beginning of the transmission, which enables combined estimation of the channel and I/Q imbalance, as expressed by (4).

The training symbol we employ is formed by a series of interleaved pilot tones and null subcarriers, so that each mirrored couple defined in (5) consists of a pilot tone and a null subcarrier. To achieve this we transmit the pilot tone only for the even-numbered subcarriers c_k in the first half of the OFDM frequency band, $1 \leq k \leq N/2$, and for odd-numbered subcarriers in the range $N/2+3 \leq k \leq N-1$. With this symbol structure and using (4), we can estimate the scaled channel frequency responses $\hat{H}_\alpha[k]$ and $\hat{H}_\beta[k]$ from the received and echo-canceled signal for half of the subcarriers as follows

$$\hat{H}_\alpha[k] = \frac{Y[k]}{X[k]},\ k = \begin{cases} 2i, & 1 \leq i \leq N/4 \\ 2i+3, & N/4 \leq i \leq N/2-2 \end{cases}$$

$$\hat{H}_\beta[k] = \frac{Y[k]}{X^{\#}[k]},\ k = \begin{cases} 2i+1, & 1 \leq i \leq N/4-1 \\ 2i+2, & N/4 \leq i \leq N/2-1 \end{cases}$$

After obtaining the estimations of $\hat{H}_\alpha[k]$ and $\hat{H}_\beta[k]$ for the subgroup of carriers, the frequency domain distortion for all subcarriers is interpolated using the method described in [16].

This estimation of the far-end channel and transmitter I/Q imbalance combined response is used to equalize in frequency domain the received symbols prior to demodulation at the receiver, and to reconstruct the far-end signal in the second stage of echo-cancellation. We suppose that the channel remains constant during the transmission of the OFDM symbol. A new estimation is necessary if the wireless channel frequency response varies after several transmitted symbols.

A performance study of this echo canceler structure is presented in the following section, with numerical results obtained after simulations.

4 EVALUATION AND SIMULATION RESULTS

For OFDM modulation we use 128 subcarriers centered around 2.4 GHz in a 20 MHz bandwidth, 126 of them transport information using Quadrature-Phase Shift Keying (QPSK) symbols, while the remaining two are null subcarriers. Simulations were run over 100 independently generated near- and far-end channel models. Considering a transmitter placed 100 times further away from the receiving antenna than the self-interferer, if both transmitters have the same power level, the interference is 80 dB stronger than the signal of interest at the receiving antenna. According to [6], it is possible to reduce more than 60 dB of interference using RF techniques, so the remaining 20 dB have to be canceled in digital domain. Thus, we test our technique with a self-interference 20 dB stronger than the signal of interest. The impulse response length of the static wireless channel used in the simulations is $L = 6$, with a power profile defined by [0, −1, −3, −9, −12, −20] dB at each of the taps. CFO has been set equal to $\Delta f = 0,3$, normalized respect to the sampling frequency $f_s = 1/T_s = N/T$, where T is the OFDM symbol duration. Transmitter I/Q parameters have been defined according to a 3% amplitude difference and 5 degrees of phase shift between In-phase and Quadrature signal branches.

Fig. 3 illustrates the BER performance obtained by the first and second echo cancellation stages. Receiver BER for an AWGN channel with no interference is also plotted. This figure shows how performance after the second iteration of the self-interference cancellation process is enhanced.

For high SNR, the performance of the canceler is limited by the interference signal power. In Fig. 4 we show the Signal-to-Interference plus Noise Ratio (SINR) curve resulting from the simulations. When the noise power is greater than the interference signal power, the SINR is close to the SNR. When the noise level decreases and SNR increases, the interference power limits the effective SNR value for the compensated signal. The resulting SINR for the received signal with no interference cancellation is also

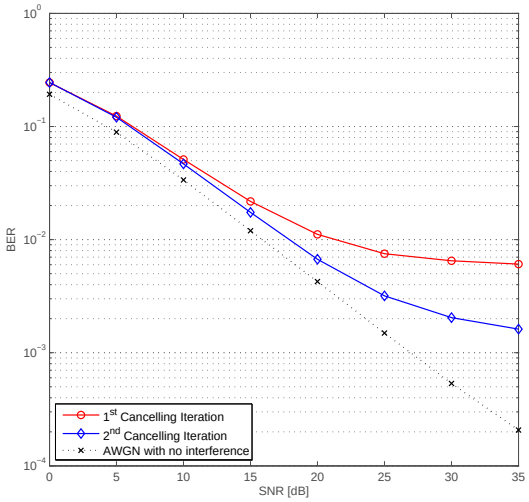

Figure 3: Bit Error Rate comparison for the two iterations of echo cancellation, and for a channel with no interference.

depicted in Fig. 4, and allows to conclude that the interference produces a high degradation to the signal of interest.

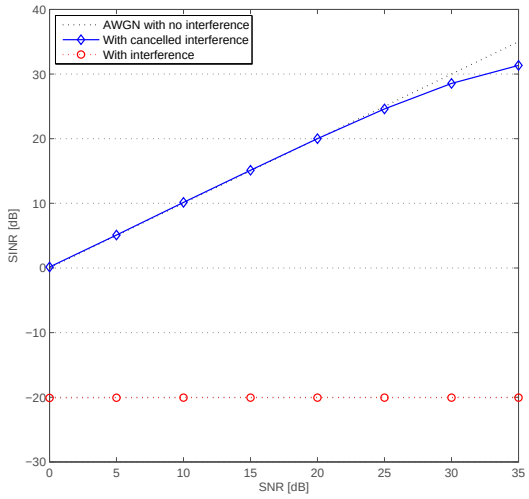

Figure 4: Signal-to-interference-plus-noise ratio obtained after echo cancellation, compared to signals with and without interference.

The mutual information achieved by a wideband transmission in a channel with limited number of dominant paths is similar to the capacity of an AWGN channel [15]. For complex symbol alphabets, this capacity is calculated as

$$C = \log_2 (1 + SNR), \qquad (13)$$

and expressed in [(bits/s)/Hz]. It is possible to obtain the capacity curves as a function of the effective SINR obtained for our system in the simulations. Considering that full-duplex operation allows transmitting twice as much information in the same time as a half-duplex system, (13) has to be scaled by a factor of two to reflect this gain. The curves obtained from our results are illustrated in Fig. 5, for a simulation with no interference and exact far-end channel and I/Q imbalance compensation, with 2-stage echo cancellation, and without interference cancellation. We can see that the echo canceler enables to achieve a system capacity curve similar to a scenario with no interference, in contrast to the null capacity obtained for a system that does not compensate the self-interference.

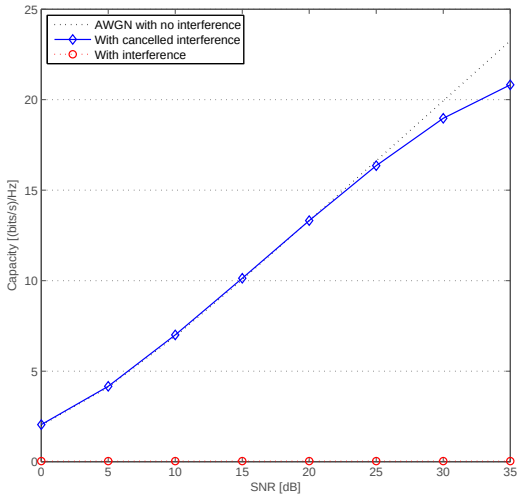

Figure 5: Capacity curves obtained for the system with echo cancellation, with interference, and without interfering signal.

5 CONCLUSIONS

In this paper, we introduced better interference models to an echo cancellation technique that enables the possibility of using a single wireless channel for full-duplex Orthogonal frequency division multiple access (OFDMA), as an alternative to OFDM-TDD or OFDM-FDD. The receiver achieves a good approximation of the interference signal, and also compensates far-end channel and transmitter degradations. This boosts the system capacity up to values close to a scenario without echo signal, opening the possibilities to increase overall throughput in current wireless communication systems.

References

[1] A. Sassan, *Mobile WiMAX : a systems approach to understanding the IEEE 802.16m radio access network*, Academic Press, 2011.

[2] H. Holma and A. Toskala, *LTE for UMTS - OFDMA and SC-FDMA Based Radio Access*, Wiley: 1st Ed, 2009.

[3] G. Fettweis, M. Lohning, D. Petrovic, M. Windisch, P. Zillmann, and W. Rave, "Dirty rf: a new paradigm," in *Proc. IEEE 16th Int. Symp. on Personal, Indoor and Mobile Radio Communications, PIMRC 2005*, Sept. 2005, vol. 4, pp. 2347–2355.

[4] M. Duarte, Full-duplex Wireless: Design, Implementation and Characterization, PhD Dissertation, Rice University, Apr. 2012.

[5] Aggarwal, V.; Duarte, M.; Sabharwal, A.; Shankaranarayanan, N.K., "Full- or half-duplex? A capacity analysis with bounded radio resources," Information Theory Workshop (ITW), 2012 IEEE, pp. 207–211, 3-7 Sept. 2012

[6] M. Jain et al., "Practical, Real-time, Full Duplex Wireless," in *Proc. of the 17th annual international conference on Mobile computing and networking*, Las Vegas, USA, 2011, pp. 301–312.

[7] J.I. Choi et al., "Achieving Single Channel, Full Duplex Wireless Communication," in *Proc. of the 16th annual international conference on Mobile computing and networking*, Chicago, USA, 2010, pp. 1–12.

[8] T. Riihonen and R. Wichman, "Analog and digital self-interference cancellation in full-duplex MIMO-OFDM transceivers with limited resolution in A/D conversion," in *Proc. of Signals, Systems and Computers (ASILOMAR) Conference*, Pacific Grove, USA, 2012, pp. 45–49.

[9] I.F. Akyildiz et al., "Enabling next generation small cells through femtorelays," *Physical Communication*, vol. 9, no. 0, pp. 1–15, 2013.

[10] E.A. Lee, and D.G. Messerschmitt, *Digital Communication*. Boston, USA: Kluwer Academic Publishers, 2nd Ed, 1994.

[11] J.G. Proakis, *Digital Communications*. New York, USA: McGraw-Hill, 4th Ed, 2001.

[12] A.F. Molisch, *Wireless Communications*. United Kingdom: Wiley, 2nd Ed, 2010.

[13] F. Luo, *Digital Front-End in Wireless Communications and Broadcasting: Circuits and Signal Processing*. New York, USA: Cambridge University Press, 2011.

[14] S. Li and R.D. Murch, "Full-Duplex Wireless Communication using Transmitter Output Based Echo Cancellation", in *Proc. of Global Telecommunications Conference (GLOBECOM 2011), IEEE*, Houston, USA, 2011, pp. 1–5.

[15] I.E. Telatar and D.N.C. Tse, "Capacity and Mutual Information of Wideband Multipath Fading Channels," *IEEE Trans. Inf. Theory*, vol. 46, no. 4, pp. 1384–1400, 2000.

[16] O. Edfors, M. Sandell, van de Beek, Jan-Jaap, S. Wilson, and P. Borjesson, "Analysis of DFT-Based Channel Estimators for OFDM," in *Wireless Personal Communications*, Kluwer Academic Publishers, vol. 12, no. 1, pp. 55-70, 2000.